Functions of a hemolysin-like protein in the cyanobacterium *Synechocystis* sp. PCC 6803

Tetsushi Sakiyama, Hiroya Araie, Iwane Suzuki, and Yoshihiro Shiraiwa*

Graduate School of Life and Environmental Sciences, University of Tsukuba, Tsukuba 305-8572, Japan

*Corresponding author

Mailing address: Graduate School of Life and Environmental Sciences, University of Tsukuba, 1-1-1 Tennodai, Tsukuba 305-8572, Japan

Phone: +81 29 853 4668

Fax: +81 29 853 6614

E-mail: emilhux@biol.tsukuba.ac.jp

Abstract

A glucose-tolerant strain of the cyanobacterium *Synechocystis* sp. PCC 6803, generally referred to as wild type, produces a hemolysin-like protein (HLP) located on the cell surface. To analyze the function of HLP, we constructed a mutant in which the *hlp* gene was disrupted. The growth rate of the mutant was reduced when the cells were stressed by treatment with $CuSO_4$, $CdCl_2$, $ZnCl_2$, ampicillin, kanamycin, or sorbitol in liquid medium, suggesting that HLP may increase cellular resistance to the inhibitory effects of these compounds. Uptake assays with $^{109}Cd^{2+}$ using the silicone–oil layer centrifugation technique revealed that both wild-type and mutant cells were labeled with $^{109}Cd^{2+}$ within 1 min. Although the total radioactivity was much higher in the wild-type cells, $^{109}Cd^{2+}$ incorporation was clearly much higher in the mutant cells after adsorbed $^{109}Cd^{2+}$ was removed from the cell surface by washing with EDTA. These findings suggest that HLP functions as a barrier against the adsorption of toxic compounds.

Keywords: cell wall; heavy metal stress; hemolysin-like protein; S-layer; cyanobacterium.

Introduction

Bacterial cells may be surrounded by a capsule composed primarily of carbohydrate polymers or by a protein surface layer (S-layer), or both (Sleytr and Messner 2000). The crystalline S-layer is the outermost cell envelope component in many bacteria and archaea. Generally, the S-layer comprises a single protein or glycoprotein and completely covers the cell surface at all stages of bacterial growth. Ranging in thickness from 5 to 25 nm, S-layers have a lattice structure exhibiting identically sized pores with diameters of 2–8 nm. S-layer proteins, ranging in apparent molecular mass from 40 to 200 kDa, are among the most abundant cellular proteins (Sleytr and Messner 2000). The middle and C-terminal regions of S-layer proteins show low sequence identity. S-layers are reported to provide prokaryotic cells with a selective advantage by functioning as a protective coating, in cell adhesion, for surface recognition, and as ion traps.

Repeat-in-toxin (RTX) proteins are exotoxins produced by Gram-negative bacteria (Ludwig 1996). RTX proteins are considered to form pores in the cytoplasmic membranes of erythrocytes, leukocytes, and other cells, leading to the modification of cellular functions and/or lysis of host cells. RTX proteins are characterized by the GGXGXDXUX nonapeptide motif (X, any amino acid; U, an amino acid with a large hydrophobic side chain), which serves as two half-sites for Ca^{2+} binding. An array of the sequences forms a parallel β-roll structure (Baumann et al. 1993). Biochemical and molecular biological studies have best characterized HlyA of *Escherichia coli* (Wiles et al. 2008).

Cyanobacteria are ubiquitous microorganisms and conduct oxygenic photosynthesis in various environments. S-layers have been observed in 60 strains of cyanobacteria (Šmarda et al. 2002). SwmA, an S-layer protein of

Synechococcus sp. WH8102, is involved in cell movement (swimming motility), and the S-layer of *Synechococcus* sp. GL24 has been reported to act as a template for fine-grain gypsum and calcite formation (Schultze-Lam et al. 1992; Brahamsha 1996). The functions of S-layers in other cyanobacteria have not been clarified.

We have reported that a glucose-tolerant (GT) strain of the cyanobacterium *Synechocystis* sp. PCC 6803, which is commonly used in studies, overproduces hemolysin-like protein (HLP) Sll1951, an RTX protein localizing in the S-layer (Sakiyama et al. 2006). However, its function is unclear. In the present study, we constructed two *sll1951* (*hlp*) mutants, namely GDkF1 and GD, and used these to analyze the function of HLP. We demonstrate that HLP protects *Synechocystis* cells from growth inhibition by heavy metals, antibiotics, and osmotic stress.

Materials and methods

Synechocystis strains and culture conditions

A GT strain of *Synechocystis* sp. PCC 6803 was used as the wild-type strain throughout this study (refering to Williams 1988). The construction of the two *hlp* mutant strains, GDkF1 and GD, is described below. These cells were grown at 30°C in BG11 medium containing 20 mM HEPES–NaOH (pH 7.5) with continuous shaking at 90 rpm on a rotary shaker and under continuous illumination provided by incandescent lamps at an intensity of 70 μmol photons $m^{-2} \cdot s^{-1}$ (Sakiyama et al. 2006). The GDkF1 and GD cells were grown in the presence of 25 $\mu g \cdot ml^{-1}$ kanamycin and spectinomycin, respectively, for the selection of mutants. *Escherichia coli* strain JM109 (TaKaRa Bio, Ohtsu, Japan) was grown in Luria–Bertani (LB) medium containing the appropriate antibiotics

at 37°C and used as a host for genetic manipulation.

To measure growth rates under various conditions, cultures of wild-type and mutant cells were initiated at OD_{750} 0.04–0.05, and the growth rate was calculated from the change in OD_{750} per hour. To test the effect of heavy metal stress, wild-type and GD mutant cells were grown separately in medium containing 0–5 μM $CuSO_4$, 0–10 μM $CdCl_2$, or 0–10 μM $ZnCl_2$. As BG11 medium usually contains 250 μM $CaCl_2$, $CaCl_2$ solution was added to Ca^{2+}-free BG11 medium to prepare the medium containing various concentrations of Ca^{2+}. To test the effect of antibiotic stress, 0–5 $\mu g \cdot ml^{-1}$ ampicillin or kanamycin was added to the medium. To test the effect of osmotic stress, 0–1 M (final concentration) sorbitol was added to the medium.

Disruption and deletion of the *hlp* gene

The *hlp* gene was disrupted by insertional mutagenesis as described previously (Williams 1988). Briefly, DNA fragments containing part of the *hlp* gene were amplified from the chromosomal DNA of wild-type cells by polymerase chain reaction (PCR) using the primers GTCGACTTTGGGACGTTTCTGAGCCC and ACTAGTTCAGAGAGTTTAGGCGTAGA for the construction of GDkF1 and CAACCTCCAAACTGCTTTGGAAACCG and ACTAGTTCAGAGAGTTTAGGCGTAGA for the construction of GD.

The PCR fragment for GDkF1 was cloned into pT7Blue (Invitrogen, Carlsbad, CA), and a kanamycin-resistant gene cassette was introduced with the EZ::TN<KAN-2> system (Epicentre, Madison, WI). The PCR fragment for the GD mutant was cloned into pT7Blue (Invitrogen), which was cut at two *Hap*I sites in the insertion sequence to substitute 2390 bp of the coding region of *sll1951* with a spectinomycin resistance cassette. The resultant plasmids were

propagated respectively in *E. coli* JM109, and the sites and direction of the inserted cassettes were confirmed by sequencing. Eight nucleotides in the coding region of *sll1951* cloned in GDkF1 were substituted from the published sequence (Kaneko et al. 1996). The *E. coli* transformants were grown at 37°C in LB medium supplemented with 25 μg·ml^{-1} kanamycin (for GDkF1) or 25 μg·ml^{-1} spectinomycin (for GD). The purified plasmids were used, respectively, to transform wild-type cells and produce the *hlp*-disrupted mutant GDkF1 and the *hlp*-deficient mutant GD (Online Resource 1) by homologous recombination (Williams 1988). The presence of the inserted cassettes in the coding region of the *hlp* gene was confirmed by PCR.

Western blot analysis

The expression of HLP in the *hlp*-mutants was evaluated by Western blot analysis. Cell proteins were separated by SDS-PAGE and electro-transferred onto a polyvinylidene fluoride membrane. Rabbit anti-HLP serum (Sakiyama et al. 2006) and peroxidase-conjugated anti-rabbit IgG (Bio-Rad, Hercules, CA) were used as primary and secondary antibodies, respectively. After blocking with 5% (w/v) bovine serum albumin in TBST buffer [50 mM Tris–HCl (pH 8.0), 150 mM NaCl, 0.05% (w/v) Tween 20], the membrane was incubated with primary antibody at 1:1,000 dilution in buffer and then with secondary antibody at 1:1,600 dilution in the same buffer. Immunoreactive HLP was detected using dianisidine solution (10 mM Tris–HCl, pH 7.5, 0.57 mM *o*-dianisidine, 1% methanol, and 1.6% H_2O_2).

Measurement of survival rate under high temperature and desiccation stresses

Wild-type and mutant cells at late-logarithmic phase (OD_{750} = 1) in liquid

culture were used for determining the survival rate under high-temperature and desiccation stresses. To test tolerance to high-temperature stress, cells in 0.5 ml of liquid culture in 1.5-ml centrifuge tubes were incubated at 40.5, 50, 55.5, 60.5, and 69.5°C in a water bath for 5 min. The initial cell numbers were 3.0×10^7 and 2.8×10^7 cells/ml for wild-type and GDkF1 cells, respectively. After incubation, the cells were treated with reagent from the Live/Dead BacLight Bacterial Viability kit (Molecular Probes, Eugene, OR). The living (green fluorescence) and dead cells (red fluorescence) were counted using a hemocytometer under an optical microscope (Eclipse E600; Nikon, Tokyo, Japan) with epifluorescence. The assays were carried out three times with the same cultures. The survival rates were calculated as the ratio of the number of living to total cells. To test tolerance to desiccation stress, cells in liquid culture at late-logarithmic phase (5 µl) were incubated and air-dried at 30°C under illumination (10 µmol photons $m^{-2} \cdot s^{-1}$) in a 1.5-ml capless tube covered with a Petri dish for 0, 1, 2, and 3 h. The initial cell numbers were 3.0×10^7 and 3.2×10^7 cells ml^{-1} for wild-type and GD mutant cells, respectively. After incubation, the numbers of living and dead cells were counted as described above. The assays were performed twice, and the survival rate was calculated as described above.

^{109}Cd uptake assay

The ^{109}Cd uptake activity was determined using the silicone–oil-layer centrifugation technique (Obata et al. 2004). First, the silicone–oil layer was prepared as a mixture of SH 550 and SH 556 at a ratio of 2:3 (Dow Corning Toray Silicone, Tokyo, Japan) in a 0.4-ml microcentrifuge tube (30-mm diameter and 115-mm length; no. 72,700; Assist, Tokyo, Japan). Then, 80 µl of the silicone–oil layer were placed at the bottom of the tube. For the ^{109}Cd uptake experiment,

300 µl of cell suspension of wild-type and GD cells were transferred from a pre-culture into a 1.5-ml centrifuge tube containing Tween 20 (final concentration, 0.05%), and the reaction was initiated by addition of 10 µl of ^{109}Cd-chloride (126.17 MBq·mg^{-1}; PerkinElmer, Waltham, MA). The numbers of wild-type and GD cells were adjusted to be the same with BG11 medium. At appropriate intervals, 200 µl of the each cell suspension were removed and layered onto the silicone–oil layer in separate microcentrifuge tubes. Then, the reaction was terminated by immediate centrifugation of the microcentrifuge tubes at 10,000 × *g* for 1 min; the cells passed through the silicone–oil layer and were separated from the reaction mixture. The tube was quickly frozen in liquid nitrogen. To determine the radioactivity in the culture medium and cell pellet, the tube was cut with a razor at the position of the silicone oil layer, and the radioactivity in each fraction was determined using a gamma counter (AccuFLEX γ7000; ALOKA, Japan). These experiments were performed three times under each condition.

Determination of cell size by flow cytometry

The sizes of the wild-type and GD cells in liquid culture at late-logarithmic phase (OD_{750} = 1) were measured by flow cytometry (FACSCalibur, Becton Dickinson, Franklin Lakes, NJ). The cells (1 ml) were diluted with 1 ml of sheath fluid solution (Becton Dickinson) and analyzed. Beads of 2 µm and 6 µm (Polysciences, Warrington, PA) were analyzed first as controls. The results were analyzed using Cell Quest software (Becton Dickinson). The FSC values (relative cell sizes) of the cells and beads were determined from histograms, and the sizes of both cell types were estimated by comparison with the FSC values of the beads.

190 Electron microscopy

191 The method for electron microscopy was according to Yubuki et al. (2007) with
192 slight modification. Cell suspensions were mixed with an equal volume of 1%
193 glutaraldehyde in sodium cacodylate buffer (0.2 M $(CH_3)_2AsO(OH)$-NaOH, pH
194 7.2) and incubated at 4°C for 2 h. After washing with cacodylate buffer, the cells
195 were fixed by incubation in 1% osmium tetroxide at 4°C for 2 h. After washing
196 with the buffer, the cells were dehydrated through a series of ethanol
197 concentrations: 50% ethanol for 1 h, followed by 75, 90, 95, and 99.5% ethanol
198 for 30 min each. For freeze-substitution fixation, the cells were fixed by
199 incubation in anhydrous acetone containing 2% osmium tetroxide at −80°C for
200 48 h, after fixation in 1% glutaraldehyde at 4°C. Then, these cells were warmed to
201 room temperature at a rate of 1°C/min with a pause at −20°C for 2 h and at 4°C
202 for 1 h, washed, and dehydrated in 99.5% anhydrous acetone for 1 h. After
203 dehydration with ethanol or anhydrous acetone, the cells were treated with a 1:1
204 mixture of 99.5% ethanol or anhydrous acetone and propylene oxide twice for 10
205 min each, and then with 99.5% propylene oxide twice for 10 min each. The
206 propylene oxide was replaced with Spurr's resin (Spurr 1969) by treatment with a
207 1:1 mixture of propylene oxide and resin, followed by treatment with the resin.
208 The resin was polymerized at 70°C for 12 h. Thin sections (50-nm thickness) were
209 cut with an ultramicrotome (EM-Ultracuts, Reichert, Germany) and stained with
210 2% uranyl acetate and lead citrate (Reynolds 1963). The samples were observed
211 under a transmission electron microscope (JEM1010; JEOL, Tokyo, Japan).
212
213

Results and discussion

Influence of *hlp* mutation on the response to heat and desiccation stresses

We first speculated that HLP protects cells against high-temperature stress, in analogy to HecA and SigB in *Synechocystis* sp. PCC 6803 (Singh et al. 2006), because we had previously found that heat treatment above 60°C changes the conformation of HLP and releases the bound Ca^{2+} (Sakiyama et al. 2006). The survival rate of wild-type cells at high temperatures of 40.5–69.5°C was almost the same as that of GDkF1 cells (Online Resource 2A and B), suggesting that HLP does not protect wild-type cells against heat stress. Furthermore, the survival rate under desiccation stress was similar between wild-type cells and GD mutant cells (Online Resource 2C and D), indicating that HLP does not function as a protectant against desiccation stress.

Influence of *hlp* mutation on the response to heavy metal stress

In a previous study, some HLP was released from the surface of wild-type cells into the culture medium when the cells were exposed to more than 3 μM $CuSO_4$ (Sakiyama et al. 2006); hence, we speculated that HLP may be involved in tolerance to metal ion stress. Retardation of the growth rate was more obvious in GD cells than in wild-type cells when the $CuSO_4$ concentration in the medium was increased (Online Resource 3A and E). In addition, the concentration of $CuSO_4$ required for 50% growth inhibition (ID_{50}) was higher for wild-type cells than for GD cells in two experiments (Table 1).

The inhibitory effect of $CdCl_2$ (above 1 μM) on the growth rate was more obvious in GD cells than in wild-type cells, and the difference became greater with time (Online Resource 3B and F). A similar inhibitory effect was observed

240 with $ZnCl_2$ at concentrations above 0.5 μM (Online Resource 3C and G).
241 Furthermore, the ID_{50} values of $CdCl_2$ and $ZnCl_2$ were higher for wild-type cells
242 than for GD cells (Table 1). These results suggest that HLP may function to
243 protect cells from heavy metal stress.

244 HLP has been shown to bind Ca^{2+} at a ratio of 100 Ca^{2+} per HLP molecule,
245 with 29 Ca^{2+} binding to one Ca^{2+}-binding motif of HLP (Sakiyama et al. 2006).
246 Assuming that HLP serves as a Ca^{2+} reservoir, we examined the effect of Ca^{2+} on
247 the growth of wild-type and GD cells. However, no effect was observed in either
248 cell line at Ca^{2+} concentrations up to 2 mM, under any conditions examined
249 (Table 1 and Online Resource 3D). These results demonstrate that HLP has no
250 function associated with calcium utilization.

251 HLP may reduce the ability of toxic metals such as Cu^{2+}, Cd^{2+}, and Zn^{2+} to
252 enter cells, given that carboxyl and phosphate groups on cell surface molecules
253 have been shown to absorb toxic metals in the cyanobacterium *Spirulina*
254 (Chojnacka et al. 2005). HLP could bind with metals via free carboxyl groups of a
255 polypeptide or attached polysaccharide. HLP does not appear to present a physical
256 barrier against non-ionic molecules, as even myoglobin can pass through the S-
257 layer (Sára et al. 1992). We speculated that in the wild-type cells of *Synechocystis*
258 sp. PCC 6803 (GT strain), the toxic influence of heavy metals is initially reduced
259 by HLP acting a diffusion barrier, and then enzymes are induced for more
260 effective detoxifying mechanisms using the two-component system of the
261 environmental stress response (Murata and Suzuki 2006). Further studies are
262 necessary to elucidate the defense system against heavy metal stress in
263 *Synechocystis* sp. PCC 6803.
264

265 Influence of *hlp* mutation on the response to antibiotics and osmotic stresses

266 The inhibitory effect of ampicillin or kanamycin on cell growth was more
267 obvious in mutant cells than in wild-type cells at ampicillin or kanamycin
268 concentrations higher than 0.1 $\mu g \cdot ml^{-1}$, and the inhibitory effect increased with
269 time (Online Resource 4A, B, D, and E). Moreover, the ID_{50} values of ampicillin
270 and kanamycin were higher in the wild-type cells than in the mutant cells at all
271 times in Exp. 1 and Exp. 2 (Table 2). These results suggest that HLP functions to
272 reduce the inhibitory effect of ampicillin and kanamycin. Polysaccharides
273 attached to HLP could form a biofilm matrix and thereby suppress the diffusion of
274 antibiotics into the cell (Silverstein and Donatucci 2003).

275 Compared with GD cell growth, the growth of wild-type cells was more
276 resistant to osmotic stress created by sorbitol (Online Resource 4C and F). The
277 ID_{50} for sorbitol was higher in wild-type cells than in mutant cells at all times in
278 Exp. 1 and Exp. 2 (Table 2). The S-layer possesses characteristics of an
279 exoskeleton and may be important for maintaining shape (Engelhardt 2007).
280 Furthermore, liposomes harboring the S-layer protein of *Bacillus*
281 *stearothermophilus* had an enhanced ability to maintain their shape against
282 mechanical stress (Mader et al. 1999). Thus, HLP may function through an
283 unknown mechanism to maintain cellular structure despite low turgor pressure in
284 *Synechocystis* sp. PCC 6803 cells, allowing time for the induction of enzymes via
285 the two-component system (Murata and Suzuki 2006). The defense system of
286 *Synechocystis* sp. PCC 6803 cells under osmotic stress needs to be clarified.

287

288 ^{109}Cd uptake by wild-type and GD mutant cells

289 To investigate the resistance of wild-type cells to the effects of heavy metals, a
290 ^{109}Cd uptake assay was performed in wild-type and GD cells. The radioactivity

291 absorbed by wild-type and GD cells reached a plateau within about 1 min in each
292 experiment (Fig. 1a). After 1 min, 90% of the radioactivity was easily removed
293 from both wild-type and GD cells by treatment with 5 mM EDTA (Experiment 2
294 in Fig. 1b), suggesting that the $^{109}Cd^{2+}$ was attached mainly on the cell surface.
295 The ~10% of the $^{109}Cd^{2+}$ that remained with the cells after EDTA treatment might
296 have been incorporated into the cells. The radioactivity level associated with wild-
297 type cells was 1.3- to 2.0-fold that associated with GD cells for the first 10 min in
298 each experiment. However, after 1500 min, the level of radioactivity was the same
299 for both wild-type and GD cells. Furthermore, the radioactivity that was removed
300 by washing with EDTA decreased less in wild-type cells than in GD cells (Fig. 1b).
301 These results indicate that while wild-type cells absorbed more Cd^{2+} than GD
302 cells, more Cd^{2+} was incorporated into GD cells than into wild-type cells. Using
303 an *in vivo* atomic absorption technique, we have previously demonstrated the
304 binding of HLP with heavy metals (Sakiyama et al. 2006). Taken together, these
305 data strongly support our proposal that HLP functions as a barrier against heavy
306 metals and other toxic compounds.

307 The sizes of the wild-type and GD cells were almost equal (2.33 ± 0.33 μm and
308 2.25 ± 0.62 μm, respectively), suggesting that the amount of extracellular material
309 did not make a difference in the binding to HLP. Liu and Curtiss (2009) showed
310 that 7 μM Ni^{2+} did not influence cell size in *Synechocystis* sp. PCC 6803. These
311 results suggest that the difference in ^{109}Cd binding between the wild-type and GD
312 cells may be explained by the presence or absence of HLP.

313 Electron micrographs showed that the wild-type cells had cell surface
314 structures and an S-layer containing a high amount of electron-dense material (Fig.
315 2a). Unfortunately, GD mutant cells aggregated during fixation with osmium
316 tetroxide at 4°C, preventing electron microscopic observation of the cell surface.

With the freeze-substitution method of fixation, the S-layer of wild-type cells was ambiguous, and that of mutant cells was not observed; no clear photographs could be taken (data not shown). McCarren et al. (2005) showed cell surface structures (cell membrane, peptidoglycan, outer membrane, and S-layer) of the cyanobacterium *Synecococcus* sp. WH8102, but no S-layer in mutant cells. Several studies of the bacterial cell surface have reported that heavy metals bind to anions of uronic acid residues of S-layer material (De Philippis et al. 2001) or anionic amino acid residues of S-layer proteins (Merroun et al. 2005; Tang et al. 2009). The evidence suggests that HLP functions in defending cells from heavy metal toxicity (Fig. 2b).

This is the first report showing that HLP functions as a barrier against various environmental and chemical stresses *in vivo*, although various functions have been reported for the S-layer in different organisms (Engelhardt 2007). Exopolysaccharides (EPS) of cells have been shown to prevent cellular access of certain antibiotics (Gilbert et al. 1997) and to sequester metals and toxins (Decho 1990; Flemming 1993). HLP in the S-layer may also function as a barrier against predators such as cyanophages and virulent bacteria. The morphological properties of the S-layer *in vivo* and the molecular nature of HLP are closely associated with HLP function. Further molecular, physiological, and morphological studies will be necessary to elucidate the functions of HLP, the S-layer, and HLP-binding polysaccharides.

Acknowledgments

We thank Dr. T. Kuwabara for his critical discussion and advice, and Dr. T. Hama and Miss M. Sawai for operation of the flow cytometer, all of whom are at the University of Tsukuba (UT). The radiolabeling experiments were performed in the

343 Radioisotope Center of UT with their kind help, especially in the ^{109}Cd uptake
344 experiments.
345
346
347

348 **References**

349

350 Baumann U, Wu S, Flaherty KM, McKay DB (1993) Three-dimensional structure
351 of the alkaline protease of *Pseudomonas aeruginosa*: a two-domain
352 protein with a calcium binding parallel beta roll motif. EMBO J. 12:3357-
353 3364

354 Brahamsha B (1996) An abundant cell-surface polypeptide is required for
355 swimming by the nonflagellated marine cyanobacterium *Synechococcus*.
356 Proceedings of the National Academy of Sciences USA 93:6504-6509

357 Chojnacka K, Chojnacki A, Górecka H (2005) Biosorption of Cr^{3+}, Cd^{2+} and Cu^{2+}
358 ions by blue-green algae *Spirulina* sp.: kinetics, equilibrium and the
359 mechanism of the process. Chemosphere 59:75-84

360 De Philippis R, Sili C, Paperi R, Vincenzini M (2001) Exopolysaccharide-
361 producing cyanobacteria and their possible exploitation: a review. Journal
362 of Applied Phycology 13:293-299

363 Decho AW (1990) Microbial exopolymer secretions in ocean environments–their
364 role(s) in food webs and marine processes. Oceanography Marine Biology
365 Annual Review 28:73-153

366 Engelhardt H (2007) Are S-layers exoskeletons? The basic function of protein
367 surface layers revisited. Journal of Structural Biology 160:115-124

368 Flemming HC (1993) Biofilms and environmental protection. Water Science and
369 Technology 27:1-10

370 Gilbert P, Das J, Foley I (1997) Biofilm susceptibility to antimicrobials. Adv Dent
371 Res 11:160-167

372 Kaneko T et al. (1996) Sequence analysis of the genome of the unicellular
373 cyanobacterium *Synechocystis* sp. strain PCC 6803. II. Sequence

374 determination of the entire genome and assignment of potential protein-
375 coding regions. DNA Res 3:109-136
376 Liu X, Curtiss R, 3rd (2009) Nickel-inducible lysis system in *Synechocystis* sp.
377 PCC 6803. Proc Natl Acad Sci USA 106:21550-21554
378 Ludwig A (1996) Cytolytic toxins from gram-negative bacteria. Microbiologia
379 12:281-296
380 Mader C, Küpcü S, Sára M, Sleytr UB (1999) Stabilizing effect of an S-layer on
381 liposomes towards thermal or mechanical stress. Biochimica et Biophysica
382 Acta 1418:106-116
383 McCarren J, Heuser J, Roth R, Yamada N, Martone M, Brahamsha B (2005)
384 Inactivation of swmA results in the loss of an outer cell layer in a
385 swimming *Synechococcus* strain. J Bacteriol 187:224-230
386 Merroun ML, Raff J, Rossberg A, Hennig C, Reich T, Selenska-Pobell S (2005)
387 Complexation of uranium by cells and S-layer sheets of *Bacillus*
388 *sphaericus* JG-A12. Applied and Environmental Microbiology 71:5532-
389 5543
390 Murata N, Suzuki I (2006) Exploitation of genomic sequences in a systematic
391 analysis to access how cyanobacteria sense environmental stress. J Exp
392 Bot 57:235-247
393 Obata T, Araie H, Shiraiwa Y (2004) Bioconcentration mechanism of selenium by
394 a coccolithophorid, *Emiliania huxleyi*. Plant and Cell Physiology 45:1434-
395 1441
396 Panoff JM, Priem B, Morvan H, Joset F (1988) Sulfated exopolysaccharides
397 produced by two unicellular strains of cyanobacteria, *Synechocystis* PCC
398 6803 and PCC 6714. Archives of Microbiology 150:558-563
399 Reynolds ES (1963) The use of lead citrate at high pH as an electron-opaque stain

in electron microscopy. J Cell Biol 17:208-212

Sakiyama T, Ueno H, Homma H, Numata O, Kuwabara T (2006) Purification and characterization of a hemolysin-like protein, Sll1951, a nontoxic member of the RTX protein family from the cyanobacterium *Synechocystis* sp. strain PCC 6803. Journal of Bacteriology 188:3535-3542

Sára M, Pum D, Sleytr UB (1992) Permeability and charge-dependent adsorption properties of the S-layer lattice from *Bacillus coagulans* E38-66. Journal of Bacteriology 174:3487-3493

Schultze-Lam S, Harauz G, Beveridge TJ (1992) Participation of a cyanobacterial S-layer in fine-grain mineral formation. Journal of Bacteriology 174:7971-7981

Silverstein A, Donatucci CF (2003) Bacterial biofilms and implantable prosthetic devices. International Journal of Impotence Research 15:S150-S154

Singh AK, Summerfield TC, Li H, Sherman LA (2006) The heat shock response in the cyanobacterium *Synechocystis* sp. strain PCC 6803 and regulation of gene expression by HrcA and SigB. Archives of Microbiology 186:273-286

Sleytr UB, Messner P (2000) Crystalline bacterial cell surface layers. In: Lederberg J (ed) Encyclopedia of Microbiology, 2nd edn. Academic Press, San Diego; London, pp 899-906

Šmarda J, Šmajs D, Komrska J, Krzyžánek V (2002) S-layers on cell walls of cyanobacteria. Micron 33:257-277

Spurr AR (1969) A low-viscosity epoxy resin embedding medium for electron microscopy. J Ultrastruct Res 26:31-43

Tang JL et al (2009) Detection of metal binding sites on functional S-layer nanoarrays using single molecule force spectroscopy. Journal of Structural

Biology 168:217-222

Vaara T (1982) The outermost surface-structures in Chroococcacean cyanobacteria. Canadian Journal of Microbiology 28:929-941

Wiles TJ, Kulesus RR, Mulvey MA (2008) Origins and virulence mechanisms of uropathogenic *Escherichia coli*. Exp Mol Pathol 85:11-19

Williams JGK (1988) Construction of specific mutations in photosystem II photosynthetic reaction center by genetic-engineering methods in *Synechocystis* 6803. Methods in Enzymology 167:766-778

Yubuki N, Inagaki Y, Nakayama T, Inouye I (2007) Ultrastructure and ribosomal RNA phylogeny of the free-living heterotrophic flagellate *Dysnectes brevis* n. gen., n. sp., a new member of the Fornicata. J Eukaryot Microbiol 54:191-200

Table 1. **Comparison of ID_{50} values of heavy metals for growth inhibition in wild-type and HLP-deficient mutant (GD) cells of *Synechocyatis* sp. PCC 6803**

The ID_{50} value, the concentration of a heavy metal required to produce 50% inhibition, was calculated from graphs of the growth rate at various concentrations of the heavy metal (see Online Resource 3). ID_{50} values were calculated from the first and second period of growth. The reported value is the average of two independent experiments.

Heavy metal	ID_{50} (μM)							
	Experiment 1				Experiment 2			
	Growth phase (h)	Wild	GD	GD/ Wild (%)	Growth phase (h)	Wild	GD	GD/ Wild (%)
Cu	0-14	3.55	2.63	74.1	0-17	7.32	3.01	41.1
	14-25	3.10	1.44	46.5	17-41	3.01	0.80	26.6
Cd	0-14	5.50	4.53	82.4	0-16	4.42	3.85	87.1
	14-25	3.46	2.21	63.9	16-62	4.36	2.56	58.7
Zn	0-20	2.25	1.30	57.8	0-16	1.73	0.92	53.2
	20-40	1.30	0.60	46.2	16-62	1.22	0.59	48.4

Table 2. Comparison of ID_{50} values of antibiotics or sorbitol for growth inhibition in wild-type and HLP-deficient mutant (GD) cells of *Synechocyatis* sp. PCC 6803

For graphs of growth rate vs. antibiotics or sorbitol, see Online Resource 4. For others, see Table 1.

	ID_{50}							
	Experiment 1				Experiment 2			
Agent	Growth phase (h)	Wild	GD	GD/ Wild (%)	Growth phase (h)	Wild	GD	GD/ Wild (%)
Ampicillin	0-17	1.56	0.70	44.9	nd	nd	nd	nd
(μg/mL)	17-41	0.16	0.10	62.5	20-40	0.17	0.08	47.1
Kanamycin	0-17	2.32	0.70	30.2	nd	nd	nd	nd
(μg/mL)	17-41	0.17	0.12	70.6	20-40	0.21	0.15	71.4
Sorbitol	0-19	0.53	0.36	67.9	0-19	0.39	0.30	76.9
(M)	19-48	0.64	0.22	34.4	19-60	0.61	0.31	50.8

nd: not determined.

Fig. 1. ^{109}Cd incorporation and absorption by wild-type and *hlp*-deleted mutant (GD) cells of *Synechocystis* sp. PCC 6803 during growth in the presence of Cd.

(a) The amount of ^{109}Cd radioactivity (cpm) associated with wild-type and GD cells after incubation for the indicated times. (b) Change in ^{109}Cd radioactivity expressed as percentage of the maximum. The maximum value in each experiment is 100%. Cells at logarithmic phase were harvested and used for a ^{109}Cd uptake assay. Arrows indicate the times at which cells were treated with 5 mM EDTA to wash off the Cd bound to the outside of the cells. Cell numbers were adjusted (Experiment 1, 1.3×10^7 cells; Experiment 2, 3.8×10^6 cells; Experiment 3, 3.6×10^6 cells) with BG11 medium. The assays were carried out three times in three cultures grown independently. The means with standard deviations are indicated in each column.

Fig. 2. Schematic model of the function of HLP in *Synechocystis* sp. PCC 6803.

(a) An electron micrograph of a wild-type cell. CM, cytoplasmic membrane; PP, periplasm; PG, peptidoglycan; OM, outer membrane. (b and c) A schematic presentation of the function of HLP in wild-type (b) and GD cells (c) under heavy metal stress. Minus (–) indicates negative charges of the carboxyl and sulfate groups in HLP and the outer membrane, as demonstrated by Panoff *et al.* (1988). Note that the S-layer protein of *Synechocystis* sp. PCC 6803 is suggested to be a hexamer *in vivo* (Vaara 1982; Šmarda et al. 2002), although the soluble form of HLP is a trimer (Sakiyama et al. 2006). Small black and gray circles represent Ca^{2+} and heavy metal ions, respectively. Heavy metal ions more easily penetrated GD cells than wild-type cells because of the absence of HLP in the former.

Fig. 1

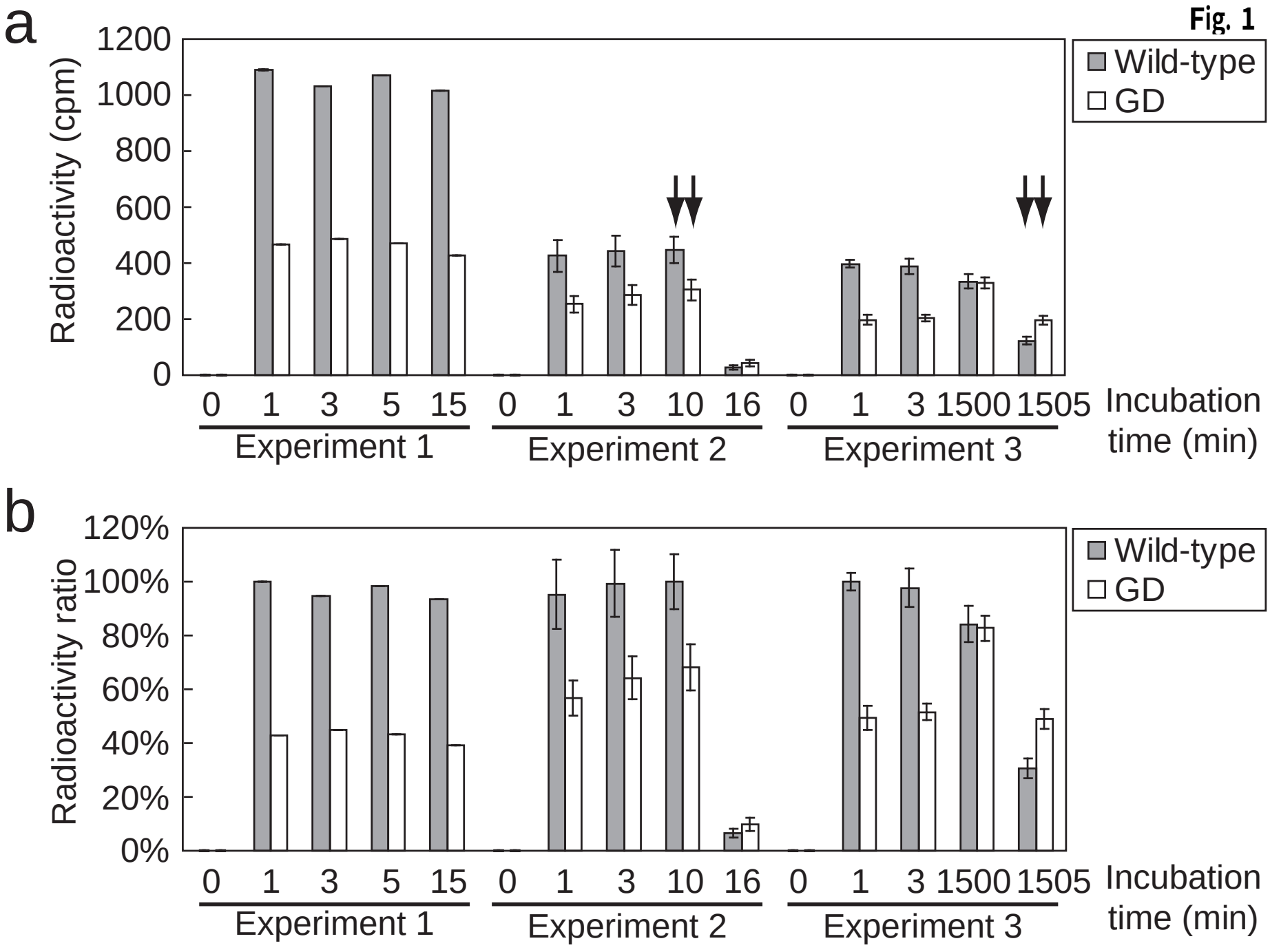
a
Radioactivity (cpm)
1200
1000
800
600
400
200
0
Wild-type
GD
0 1 3 5 15 0 1 3 10 16 0 1 3 1500 1505
Incubation time (min)
Experiment 1
Experiment 2
Experiment 3
b
Radioactivity ratio
120%
100%
80%
60%
40%
20%
0%
Wild-type
GD
0 1 3 5 15 0 1 3 10 16 0 1 3 1500 1505
Incubation time (min)
Experiment 1
Experiment 2
Experiment 3

a

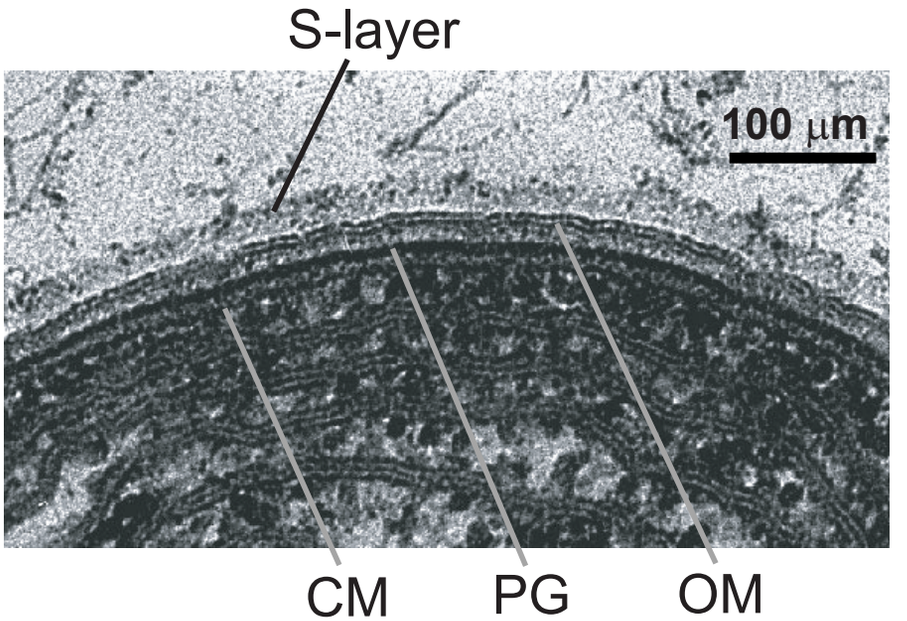
S-layer
100 μm
CM
PG
OM

b

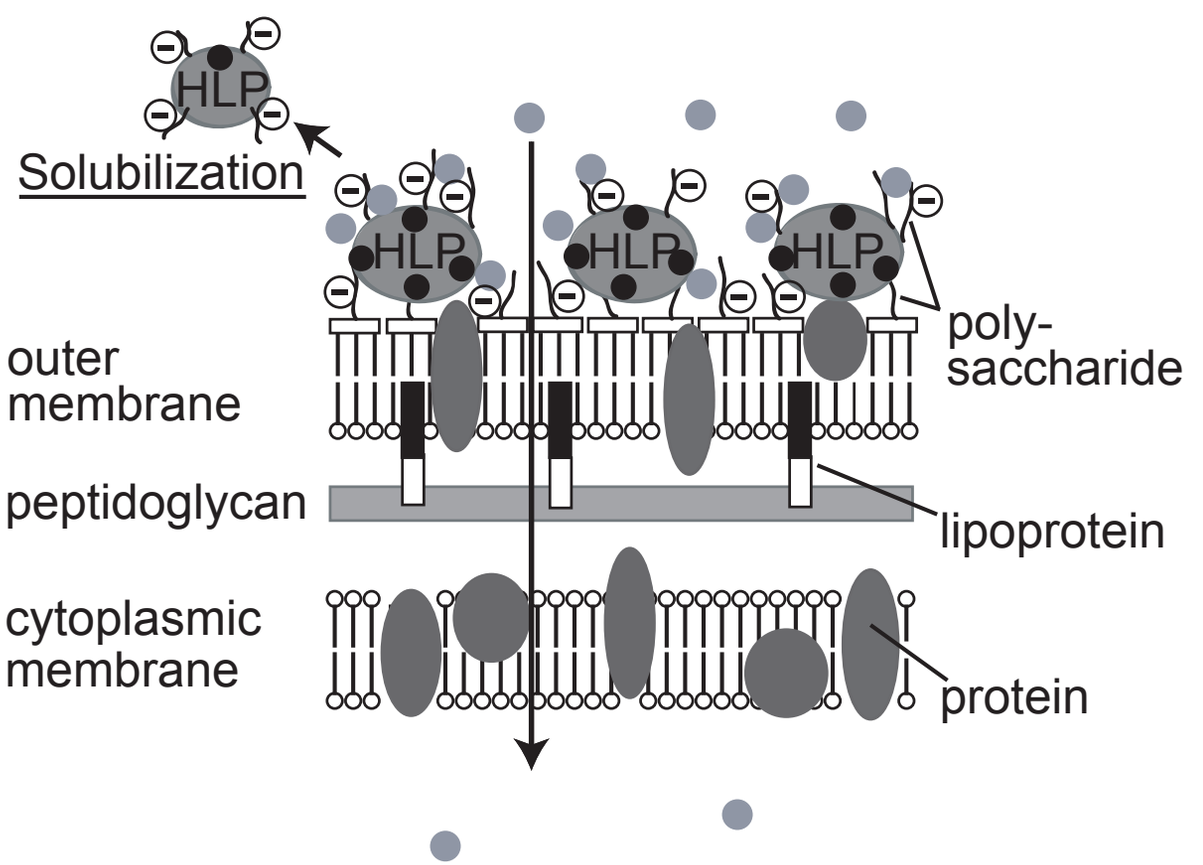
HLP
Solubilization
HLP
HLP
HLP
poly-
saccharide
outer
membrane
peptidoglycan
lipoprotein
cytoplasmic
membrane
protein

c

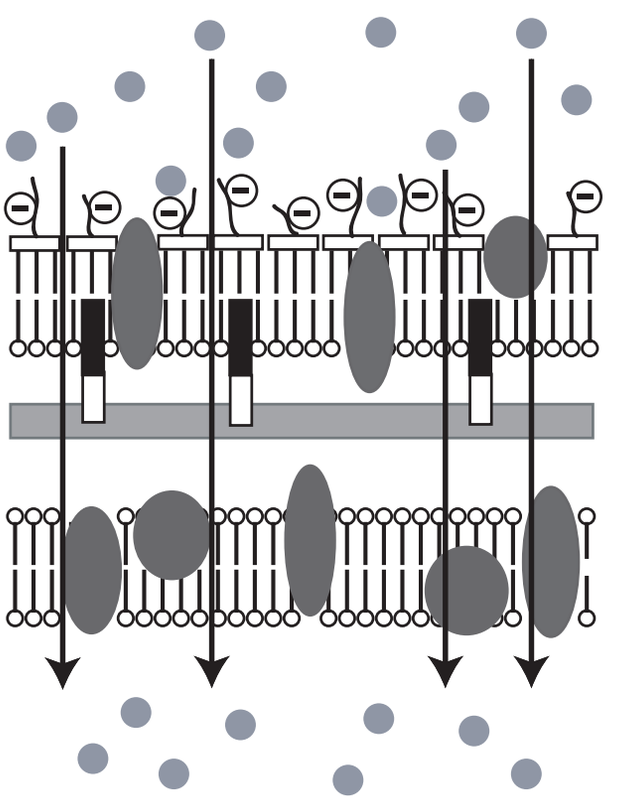

Functions of a hemolysin-like protein in the cyanobacterium *Synechocystis* sp. PCC6803

Journal name: *Archives of Microbiology*

Tetsushi Sakiyama, Hiroya Araie, Iwane Suzuki, and Yoshihiro Shiraiwa*

Graduate School of Life and Environmental Sciences, University of Tsukuba, Tsukuba 305-8572, Japan

*Corresponding author

Mailing address: Graduate School of Life and Environmental Sciences, University of Tsukuba, 1-1-1 Tennoudai, Tsukuba 305-8572, Japan

E-mail: emilhux@biol.tsukuba.ac.jp

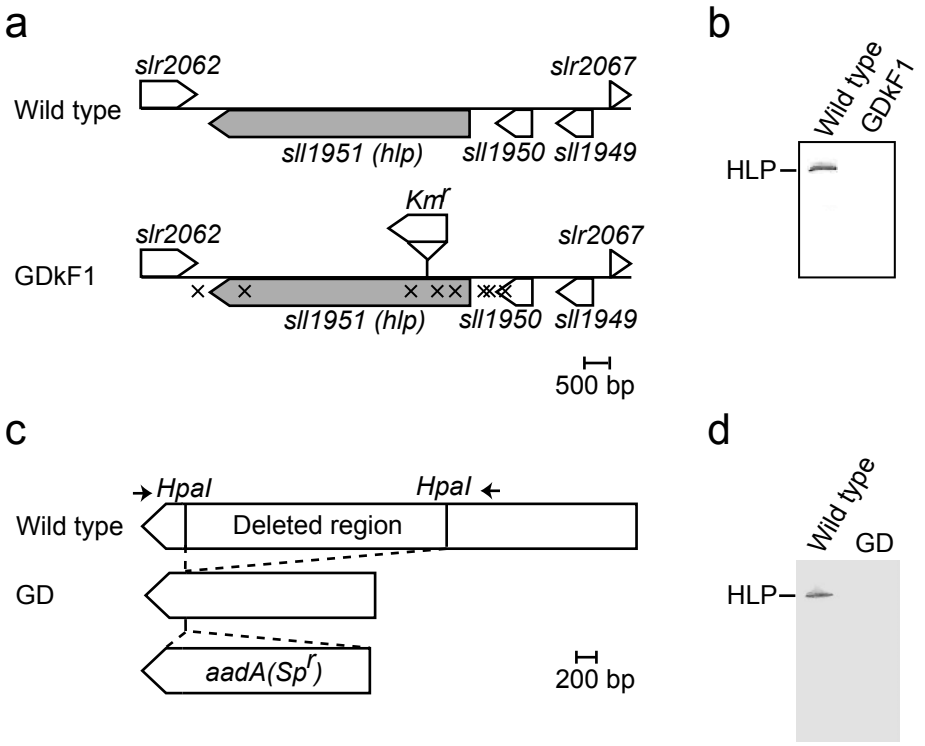

Online Resource 1 Constructs of *hlp* mutants and Western blotting profiles of HLP produced by wild-type and its hlp mutants of *Synechocystis* sp. PCC6803.

ORF of *sll1951* in wild-type cells and the *hlp*-modified GDkF1 (a) and *hlp*-deleted GD (c) mutants. Each " X " in (a) indicates a sequence that is different from the wild-type. The arrows in the directions of right and left represent the forward and reverse primers, respectively.

Km^r, kanamycin-resistance cassette; *aadA*, spectinomycin-resistance cassette; *Sp*, spectinomycin.

(b, d) Western blot profiles of proteins detected by the anti-antibody of HLP produced by wild-type cells in wild-type (b, d), GDkF1 (b) and GD cells (d).

Cell extracts containing 5 μg Chl *a* from each cell were loaded onto SDS-PAGE.

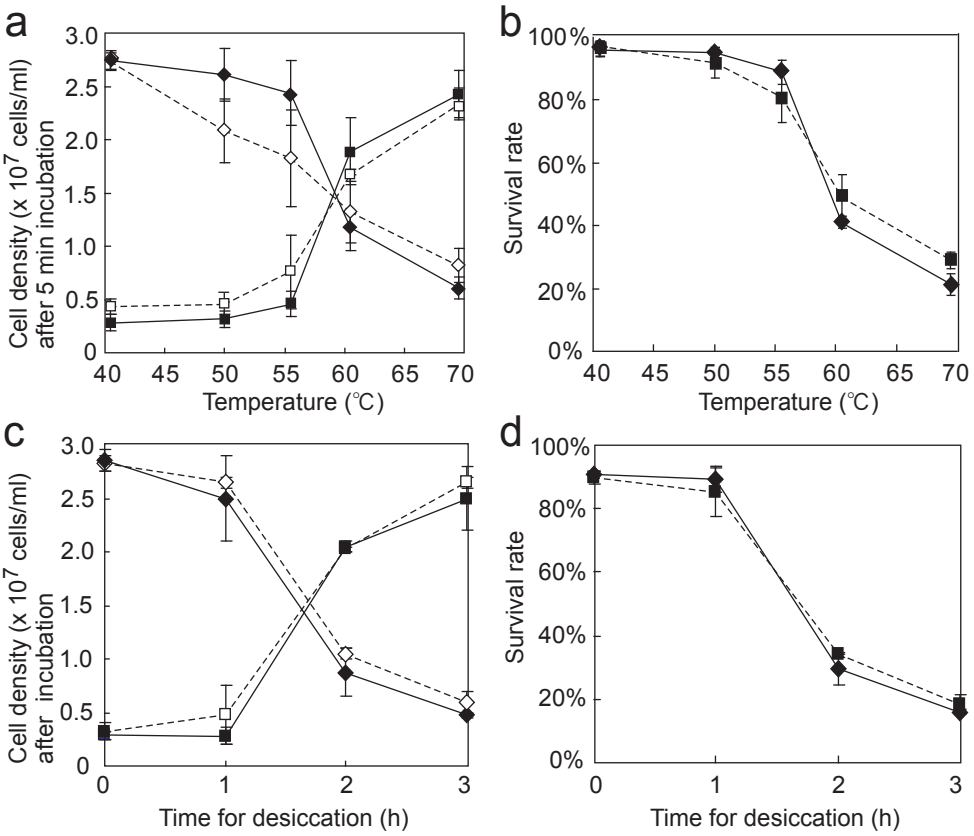

Online Resource 2 Comparison of growth and survival of *Synechocystis* sp. PCC6803 in response to various temperatures and desiccation.

The densities of dead or alive cells of wild-type and an *hlp*-modified mutant (GDkF1) after 5 min incubation at various temperatures (a) and in response to desiccation (c), respectively. Living wild-type cells (◆) and living GDkF1 cells (◇), dead wild-type cells (■) and dead GDkF1 cells (□). The survival rate of wild-type (◆) and GDkF1 (■) cells in response to various temperatures (b) and in response to desiccation (d). The survival rates were calculated from the ratios of living cells to total cells presented in (a) and (c). The assays were carried out three times with the same culture. Bars indicate means ±SEM.

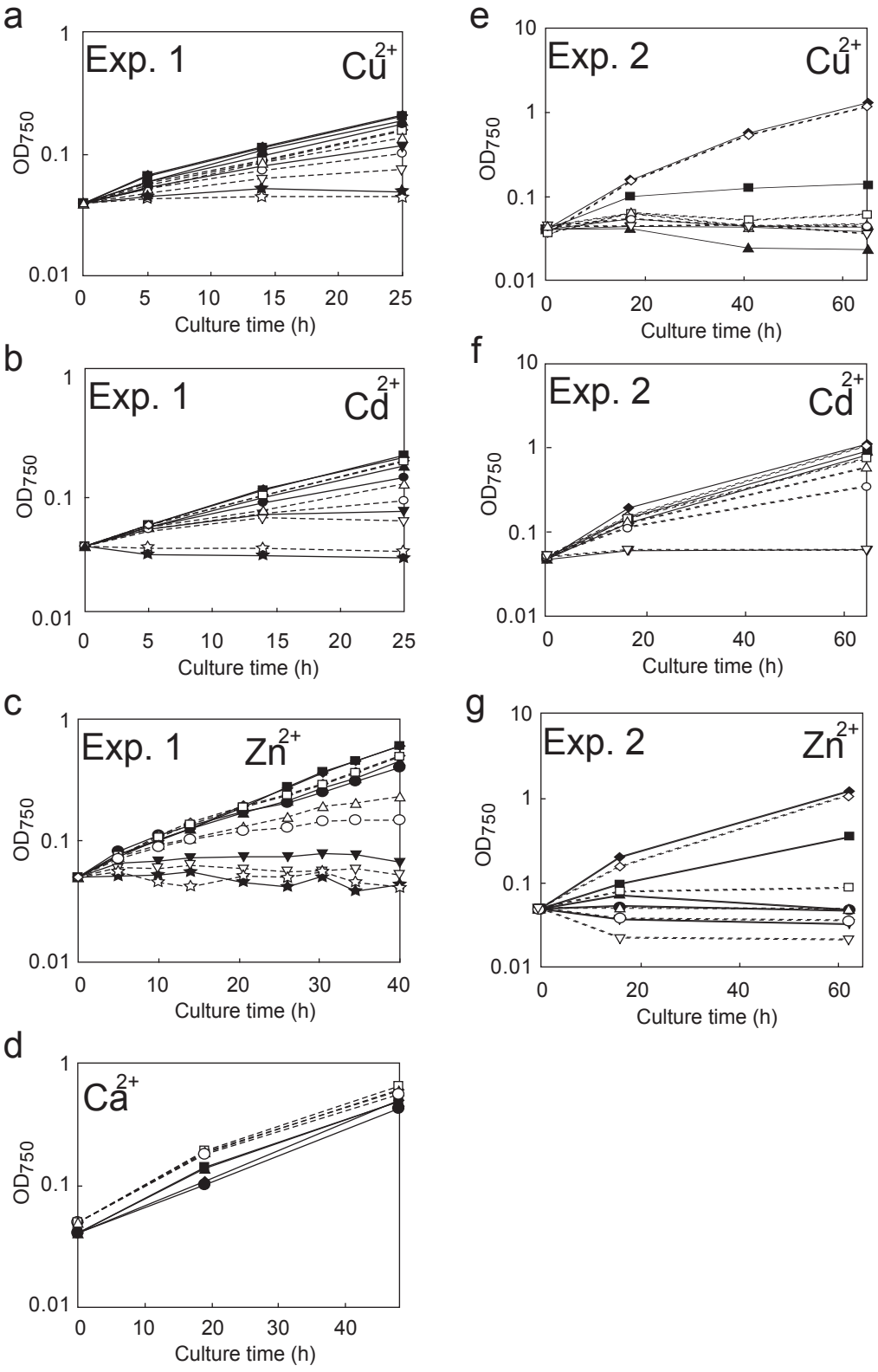

Online Resource 3 Comparison of growth of wild-type and an *hlp*-deficient mutant of *Synechocystis* sp. PCC6803 on various metal stresses.

The growth of wild-type (filled symbol) and the *hlp*-deleted (GD) mutant (blank symbol) cells were determined in the absence or presence of various concentrations of metals. Remarks are as follows: (a), $CuSO_4$ at 0 (◆),0.1 (■), 0.3 (▲), 1 (●), 3 (▼) and 5 μM (★); (b), $CdCl_2$ at 0 (◆),0.1 (■), 1 (▲), 3 (●), 5 (▼) and 10 μM (★); (c), $ZnCl_2$ at 0 (◆),0.1 (■), 0.5 (▲), 1 (●), 3 (▼) and 10 μM (★); (d), $CaCl_2$ at 0 (◆), 50 (■), 250 (▲) and 2,000 μM (●); (e), $CuSO_4$ at 0 (◆),5 (■), 10 (▲), 20 (●) and 40 μM (▼); (f), $CdCl_2$ at 0 (◆), 0.5 (■), 1 (▲), 3 (●) and 10 μM (▼); (g), $ZnCl_2$ at 0 (◆),1 (■), 3 (▲), 10 (●) and 30 μM (▼).

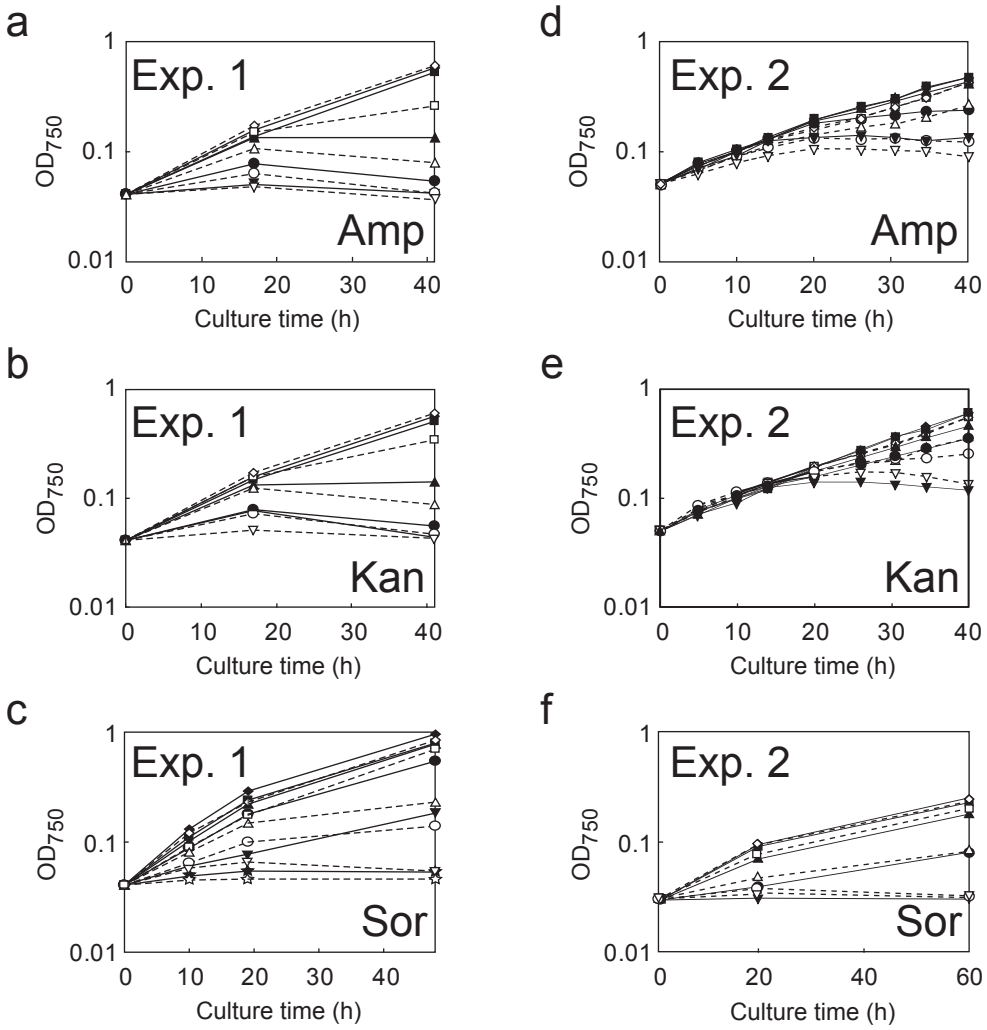

Online Resource 4 Comparison of growth of wild-type and an *hlp*-deficient mutant of *Synechocystis* sp. PCC6803 on antibiotics and an osmotic stresses.

The growth of wild-type (filled symbol) and an *hlp*-deleted (GD) mutant (blank symbol) cells were determined in the absence or presence of various concentrations of either antibiotics or sorbitol as an osmoregulant. Remarks are as follows: (a), ampicillin at 0 (◆), 0.1 (■), 0.3 (▲), 1 (●) and 5 μg/ml (▼); (b), kanamycin at 0 (◆), 0.1 (■), 0.3 (▲), 1 (●) and 5 μg/ml (▼); (c), sorbitol at 0 (◆), 0.1 (■), 0.2 (▲), 0.3 (●), 0.5 (▼) and 1 M (★); (d), ampicillin at 0 (◆), 0.01 (■), 0.1 (▲), 0.2 (●) and 0.3 μg/ml (▼); (e), kanamycin at 0 (◆), 0.01 (■), 0.1 (▲), 0.2 (●) and 0.3 μg/ml (▼); (f), sorbitol at 0 (◆), 0.1 (■), 0.3 (▲), 0.5 (●) and 1 M (▼).